Published in final edited form as:
Science. 2003 May 30; 300(5624): 1430–1434. doi:10.1126/science.1081919.

Disruption of the Epithelial Apical-Junctional Complex by *Helicobacter pylori* CagA

Manuel R. Amieva[1,2,*,†], **Roger Vogelmann**[3,*], **Antonello Covacci**[5], **Lucy S. Tompkins**[1,4], **W. James Nelson**[3], and **Stanley Falkow**[1,4]

[1]Department of Microbiology and Immunology, Stanford University School of Medicine, Stanford, CA 94305, USA

[2]Department of Pediatrics, Stanford University School of Medicine, Stanford, CA 94305, USA

[3]Department of Molecular and Cellular Physiology, Stanford University School of Medicine, Stanford, CA 94305, USA

[4]Department of Medicine, Stanford University School of Medicine, Stanford, CA 94305, USA

[5]Istituto Ricerche Immunobiologiche Siena–Chiron Vaccines, via Fiorentina 1, 53100 Siena, Italy

Abstract

Helicobacter pylori translocates the protein CagA into gastric epithelial cells and has been linked to peptic ulcer disease and gastric carcinoma. We show that injected CagA associates with the epithelial tight-junction scaffolding protein ZO-1 and the transmembrane protein junctional adhesion molecule, causing an ectopic assembly of tight-junction components at sites of bacterial attachment, and altering the composition and function of the apical-junctional complex. Long-term CagA delivery to polarized epithelia caused a disruption of the epithelial barrier function and dysplastic alterations in epithelial cell morphology. CagA appears to target *H.pylori* to host cell intercellular junctions and to disrupt junction-mediated functions.

Infection of the stomach by *Helicobacter pylori* strains containing the *cag* pathogenicity island, a type IV secretion system (TFSS), results in translocation of CagA protein into host epithelial cells and increases the risk of gastric diseases (1–4). *H. pylori* adhere to cells in the immediate vicinity of the apical-junctional complex, but the significance of this localization for pathogenesis is unclear (5, 6). The epithelial apical-junctional complex forms a network of transmembrane, scaffolding, and signaling proteins, and serves as a barrier, adhesion site, and signaling complex to control cell polarity, proliferation, and differentiation. Dysfunction of the apical-junctional complex is characteristic of many human diseases, including carcinogenesis (7–9).

To study the effects of *H. pylori* attachment to, and CagA translocation into, polarized epithelia, we developed a system of *H. pylori* infection of polarized cell monolayers Madin-Darby canine kidney (MDCK) cells (fig. S1). As observed with human infection, MDCK-adapted *H. pylori* (G27-MA) preferentially attached near cell-cell junctions (Fig. 1) (10).

[†]To whom correspondence should be addressed. amieva@stanford.edu.
[*]These authors contributed equally to this work.

Supporting Online Material
www.sciencemag.org/cgi/content/full/300/5624/1430/DC1
Materials and Methods
Figs. S1 and S2
Tables S1 and S2
References

Bacteria not only preferentially targeted the junctions, but also recruited the tight-junction scaffolding protein ZO-1 to sites of attachment (Fig. 1B), and modified the distribution of ZO-1 near junctions, suggesting an interaction between bacterial factors and host proteins (Fig. 1C).

Because CagA affects cytoskeletal organization once injected into host cells (11), we explored whether it is required to recruit ZO-1 to adherent bacteria. In MDCK cells, isogenic mutants lacking CagA (ΔCagA) adhere to the cell surface, but they adhere less frequently to junctions (fig. S1). We therefore tested wild-type and Δ*cagA* mutants for ZO-1 recruitment in cells that form organized tight junctions (MDCK cells), and in gastric adenocarcinoma cells (AGS) that express ZO-1 but are unable to form tight junctions. Wild-type *H. pylori* caused ectopic patches of ZO-1 to assemble underneath adherent bacteria in both cells (Figs. 1, B and C, and 2A). The Δ*cagA* strain readily attached to the cells but did not induce ZO-1 redistribution (ΔCagA in Fig. 2B and fig. S1). Genetic reconstitution of the *cagA* gene in the Δ*cagA* mutant rescued bacterial recruitment of ZO-1 (CagA* in Fig. 2B). Delivery of CagA to the host cell through the *cag* TFSS (12, 13) was necessary for association with ZO-1 because mutants that cannot translocate CagA [Δ*virB10* (*cag7*) or Δ*virB4* (*cag23*, *cagE*)], were unable to recruit ZO-1 to cell attachment sites (fig. S2). Simultaneous visualization of CagA, ZO-1, and *H. pylori* showed that injected CagA colocalized with ZO-1 at sites of bacterial attachment, as well as at cell-cell contacts (Fig. 2C).

Once translocated into host cells, CagA is phosphorylated by kinases of the Src family at tyrosines within the repeated five–amino acid–motif EPIYA (14, 15, 16). *H. pylori* colocalization with ZO-1 was independent of this modification because a mutant form of CagA that lacks the phosphorylation domains also induced recruitment of ZO-1 [EPISA (14) in Fig. 2B] (15). Phosphorylated CagA binds the phosphotyrosine phosphatase SHP2 as well as the adaptor protein Grb2, and these signaling events correlate with cell elongation (17, 18). CagA colocalization with ZO-1 occurs independently of cell elongation, because the $CagA_{EPISA}$ mutant recruited ZO-1 but had no effect on AGS cellular morphology (EPISA in Fig. 2B), and wild-type *H. pylori* colocalized with ZO-1 before cell elongation (Fig. 2A). Thus, CagA may mediate its effects on host cells through at least two functional domains: one that interacts with SH2 domain–containing proteins and another that interacts with components of the apical-junctional complex.

To determine whether CagA affects the barrier function of the apical-junctional complex, we used ruthenium red staining and transmission electron microscopy to examine individual junctions (Fig. 3) (10). In uninfected MDCK monolayers, tight junctions were functional as judged by the exclusion of apically applied ruthenium red from the basal-lateral space. In MDCK monolayers infected with wild-type *H. pylori*, individual junctions showed barrier dysfunction with leakage of ruthenium red into the basal-lateral space (Fig. 3B, right panel). Leakage of solutes (bovine serum albumin–biotin) across the whole monolayer was also detected in infected cells (Fig. 3A). Solute leakage across an epithelium has been described as a consequence of the *H. pylori* toxin VacA (19). Long-term infection with *H. pylori* mutants that lacked either CagA or VacA caused solute leakage across MDCK monolayers, but a double mutant lacking both CagA and VacA had intact barrier function, suggesting that both CagA and VacA alter tight-junction function (Fig. 3A). A clear effect of CagA on tight-junction organization was revealed in MDCK monolayers that were infected during synchronized junction formation (10), because wild-type *H. pylori*, not ΔCagA mutants, prevented the formation of functional tight junctions (Fig. 3C).

Because the apical-junctional complex controls cell polarity (7), we asked whether *H. pylori* infection of MDCK cells disrupts epithelial morphology. At short times after the infection of

polarized monolayers (24 hours), overt changes in MDCK cell morphology or behavior were not observed. However, after several days of infection, MDCK cells elongated and extended processes between adjacent cells, resulting in dysplastic cell shapes (Fig. 4, C and D). Intra-epithelial dysplasia depended on the injection of CagA and was reversible if monolayers were treated with antibiotics (20). Infection with an isogenic Δ*cagA* mutant over the same period caused some cellular enlargement but not dramatic effects on cell shape (Fig. 4B).

We next examined whether CagA affects the molecular organization of the apical-junctional complex. Membranes from infected MDCK cells were isolated and fractionated in iodixanol density gradients, which resolved distinct membrane fractions containing intercellular junctions, apical and basal-lateral membranes, and cytosolic proteins (10, 21). In uninfected cells and cells infected with a ΔCagA mutant, ZO-1 sediments with membranes in a narrow peak between fractions 10 and 12 (1.09 to 1.108 g/ml) (Fig. 4E). However, membranes containing ZO-1 from cells infected with wild-type *H. pylori* have a broader distribution between fractions 8 and 18 (1.071 to 1.176 g/ml), and also contained CagA (Fig. 4E). The cytoplasmic phosphatase SHP2 was weakly present or not present in membrane fractions containing apical-junctional proteins in control and Δ*cagA*-infected MDCK monolayers. In contrast, infection with wild-type *H. pylori* caused a shift in SHP2 distribution into membrane fractions containing CagA and ZO-1 (Fig. 4E). Not all tight-junction protein distributions were changed; the sedimentation profiles of the tight-junction membrane proteins occludin and claudin-1 (22) were similar in Δ*cagA* and wild-type infected cells (Fig. 4E).

This analytical method also revealed the involvement of the transmembrane protein junctional adhesion molecule (JAM) in the tight-junction protein complexes induced by CagA. In wild-type–infected MDCK monolayers, JAM distribution shifted from the lower density fractions (1.19 to 1.23 g/ml) to the fractions containing CagA (Fig. 4E). We confirmed an association between adherent bacteria, ZO-1, and JAM by confocal immunofluorescence microscopy of infected AGS cells (Fig. 4F).

Although AGS cells rapidly elongated in response to infection, polarized MDCK cells did not show morphological changes for several days. We hypothesized that the slower effect of CagA on polarized MDCK cells occurs because ZO-1 is sequestered in stable multiprotein complexes in the tight junctions, whereas in AGS cells ZO-1 is not assembled into tight junctions. To test this, we infected MDCK cells during the development of the apical-junctional complex, when individual proteins are available before their assembly into complexes (10). CagA interfered with the assembly of functional tight junctions (Fig. 3C) and altered the composition of junctional protein complexes. As early as 6 hours after infection with wild-type *H. pylori*, membranes containing ZO-1 cofractionated with phosphorylated CagA in two distinct density peaks (Fig. 4G; 6 hours, represented by the solid and dashed lines). The peak of lighter membranes (solid line) contained less ZO-1 than that from cells infected with ΔCagA *H. pylori* (Fig. 4F; 36 versus 53%, respectively, after 6 hours). After 20 hours of infection, the CagA-dependent difference in ZO-1 distribution was exacerbated. Whereas in ΔCagA-infected cells, most of the ZO-1 was found in the lighter membrane peak, the majority of ZO-1 in wild-type–infected MDCK cells fractionated in a denser peak (dashed line). Furthermore, in wild-type–infected MDCK cells, but not in uninfected or ΔCagA infected cells, a broader third peak containing phosphorylated CagA and ZO-1 appeared at a higher density. The pattern of ZO-1 fractionation in cells infected with ΔCagA *H. pylori* was similar to that of uninfected controls. The shifts in ZO-1 density fractionation seen with wild-type infection are likely the result of aberrant formation of the apical-junction protein complex, induced by CagA delivery, and could be responsible for the observed defects in barrier function and cell polarity.

H. pylori infection and CagA translocation into a tight polarized epithelium target the apical-junctional complex and are linked directly to changes in the structure, function, and morphology of these cells. CagA-mediated recruitment of the scaffolding protein ZO-1 and the tight-junction protein JAM to sites of bacteria attachment on host cell membranes may help to target and retain *H. pylori* at epithelial cell-cell junctions. Localization of signaling molecules, such as SHP2 and Src to CagA in close proximity to the tight junction may alter apical-junctional complex function (23, 24). In addition, we have previously found CagA translocation–dependent changes in gene expression of tight-junction genes in *H. pylori*–infected AGS cells (25). One consequence of long-term *H. pylori* infection with CagA+ strains, but not CagA− strains, is a greatly increased likelihood of serious noninfectious sequelae, particularly peptic ulcer disease and gastric cancer. Learning how the long-term disruption of normal apical-junctional complex signaling by CagA could be responsible for these subsequent cellular changes can teach us as much about human biology as it does about the pathogenesis of *H. pylori* infection.

Supplementary Material

Refer to Web version on PubMed Central for supplementary material.

Acknowledgments

Supported by a Pediatric Infections Disease Society of America/St. Jude Fellowship in Pediatric Infectious Diseases (M.R.A.); a Walter V. and Idun Y. Berry Fellowship (R.V.); Deutsche Forschungsgemeinschaft Fellowship VO 864/1-1 (R.V.); and NIH grants DDC DK56339 (R.V., W.J.N., and S.F.), RO1GM35227 (W.J.N.), and AI38459 and CA92229 (S.F. and L.T). We thank T. McDaniels for the use of green fluorescent protein (GFP)–expressing *H. pylori*, F. Bagnioli and M. Goodrich for DNA constructs, S. Censini for the CagA polyclonal antibody, and C. Parkos for the JAM monoclonal antibody.

References and Notes

1. Peek RM Jr, et al. Lab Invest. 1995; 73:760. [PubMed: 8558837]
2. Blaser MJ, et al. Cancer Res. 1995; 55:2111. [PubMed: 7743510]
3. Stein M, Rappuoli R, Covacci A. Proc Natl Acad Sci USA. 2000; 97:1263. [PubMed: 10655519]
4. Odenbreit S, et al. Science. 2000; 287:1497. [PubMed: 10688800]
5. Steer HW. Gut. 1984; 25:1203. [PubMed: 6500361]
6. Hazell SL, Lee A, Brady L, Hennessy W. J Infect Dis. 1986; 153:658. [PubMed: 3950447]
7. Knust E, Bossinger O. Science. 2002; 298:1955. [PubMed: 12471248]
8. Jamora C, Fuchs E. Nature Cell Biol. 2002; 4:E101. [PubMed: 11944044]
9. Bilder D, Li M, Perrimon N. Science. 2000; 289:113. [PubMed: 10884224]
10. Materials and methods are available as supporting material on *Science* Online.
11. Segal ED, Cha J, Lo J, Falkow S, Tompkins LS. Proc Natl Acad Sci USA. 1999; 96:14559. [PubMed: 10588744]
12. Fischer W, et al. Mol Microbiol. 2001; 42:1337. [PubMed: 11886563]
13. Censini S, et al. Proc Natl Acad Sci USA. 1996; 93:14648. [PubMed: 8962108]
14. Single-letter abbreviations for the amino acid residues are as follows: A, Ala; E, Glu; I, Ile; P, Pro; S. Ser; and Y, Tyr.
15. Stein M, et al. Mol Microbiol. 2002; 43:971. [PubMed: 11929545]
16. Selbach M, Moese S, Hauck CR, Meyer TF, Backert S. J Biol Chem. 2002; 277:6775. [PubMed: 11788577]
17. Higashi H, et al. Science. 2002; 295:683. [PubMed: 11743164]
18. Mimuro H, et al. Mol Cell. 2002; 10:745. [PubMed: 12419219]
19. Papini E, et al. J Clin Invest. 1998; 102:813. [PubMed: 9710450]

20. Gentamicin (10μg/ml) in the media for 3 days eliminated viable *H. pylori* from the coculture media, and MDCK cell morphology reverted to normal.

21. Yeaman C, Grindstaff KK, Wright JR, Nelson WJ. J Cell Biol. 2001; 155:593. [PubMed: 11696560]

22. Amieva MR, et al. unpublished data.

23. Collares-Buzato CB, Jepson MA, Simmons NL, Hirst BH. Eur J Cell Biol. 1998; 76:85. [PubMed: 9696347]

24. Nunbhakdi-Craig V, et al. J Cell Biol. 2002; 158:967. [PubMed: 12196510]

25. Guillemin K, Salama NR, Tompkins LS, Falkow S. Proc Natl Acad Sci USA. 2002; 99:15136. [PubMed: 12411577]

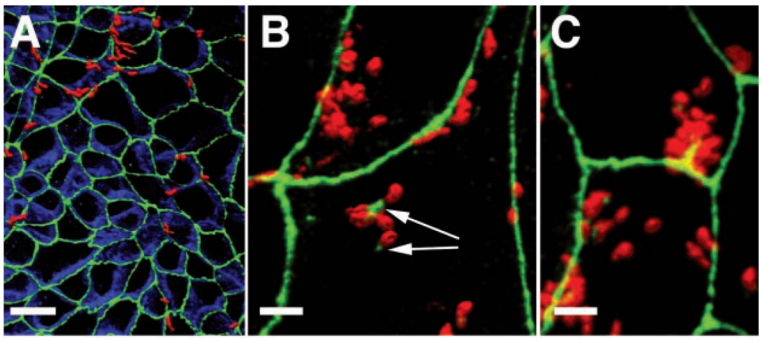

Fig. 1.

H. pylori associate with apical junctions of MDCK cells and alter the localization of tight-junction–associated proteins. Confocal immunofluorescence three-dimensional (3D) reconstructions of MDCK monolayers infected with *H. pylori* for 4 hours (**A**) or 8 hours (**B** and **C**), and stained with antibodies to ZO-1 (green), E-cadherin (blue), and *H. pylori* (red) are shown. Yellow areas indicate spatial overlap (colocalization) of the red-stained bacteria with the green ZO-1 signal. Arrows show ZO-1 recruited to extrajunctional sites of bacterial attachment in MDCK cells. Scale bar, 10 μm in (A) and 5 μm in (B) and (C).

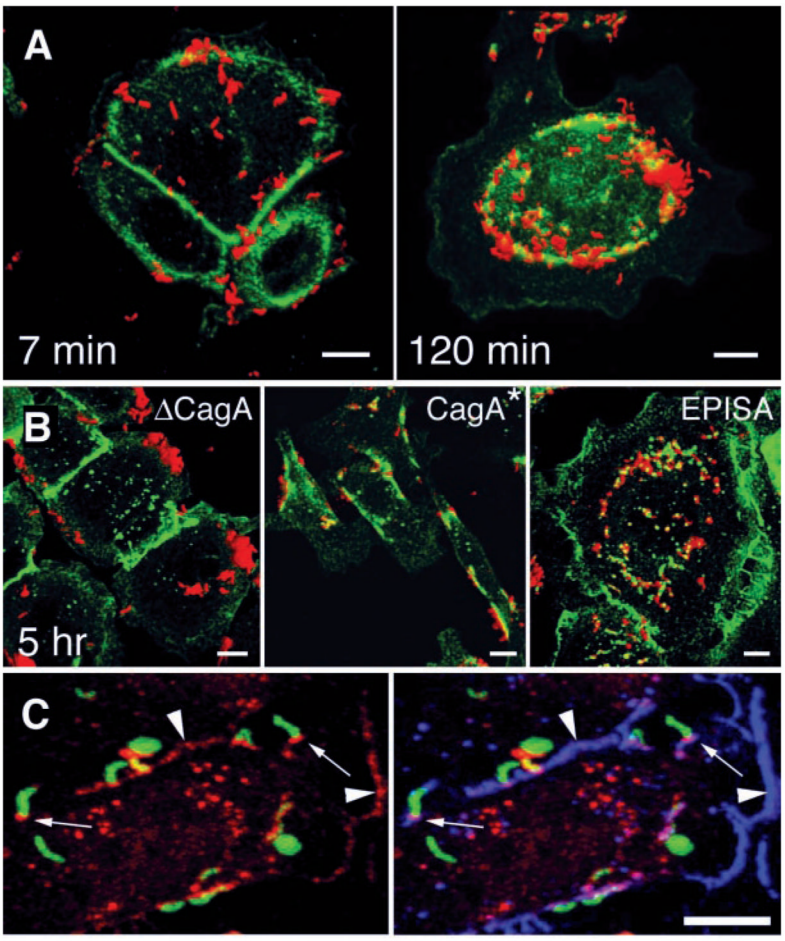

Fig. 2.

CagA is required for colocalization of *H. pylori* and the tight-junction protein ZO-1. [(A) and (B)] Confocal immunofluorescence 3D reconstructions of AGS cells infected with wild-type *H. pylori* and isogenic mutants, and stained with antibodies to *H. pylori* (red) and ZO-1 (green). (**A**) AGS cells were infected for 5 min with *H. pylori*, washed, and incubated for 7 or 120 min before fixation and staining. (**B**) AGS cells were incubated for 5 hours with an isogenic mutant lacking the *cagA* gene (ΔCagA), with wild-type reconstituted strain G27 CagA*, and with a mutant expressing a form of CagA that cannot be phosphorylated in tyrosine residues (EPISA). (**C**) Confocal immunofluorescence 3D reconstructions of AGS cells infected for 2 hours with *H. pylori* and modified to express GFP (green), and stained with antibodies to CagA (red) and ZO-1 (blue). Yellow represents areas of GFP and CagA colocalization, which are especially intense in some bacteria that became permeabilized to the antibodies during the staining. Colocalization of CagA and ZO-1 is present at sites of bacterial attachment (small arrows) and at cell-cell contact sites (arrowheads). Scale bar, 5 μm.

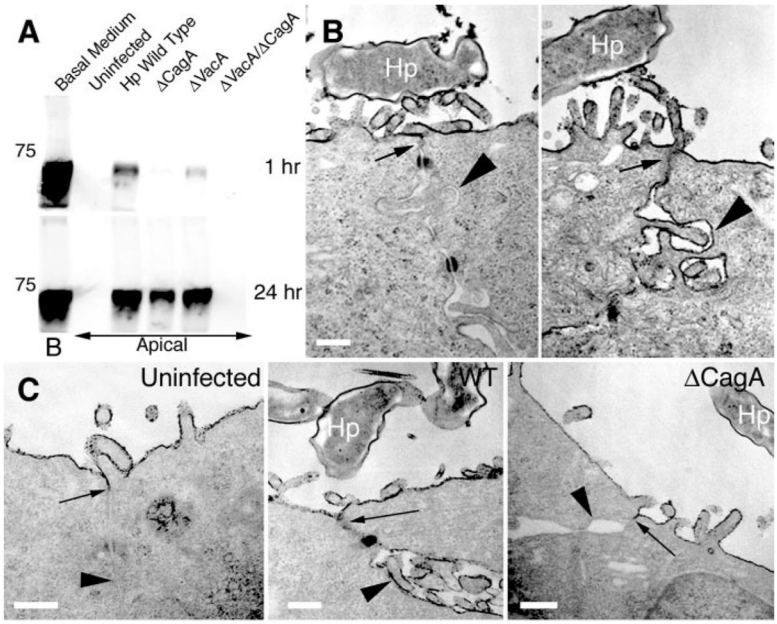

Fig. 3.

Infection of MDCK monolayers with *H. pylori* causes disruption of tight-junction barrier function and prevents normal junction formation. (**A**) Diffusion of biotinylated albumin across infected MDCK monolayers. Confluent monolayers on Transwell filters were infected with *H. pylori* or isogenic mutants in the apical chamber. At day 10 after infection, media in the basolateral chambers were marked with biotinylated albumin (Basal Medium, B) and samples were collected 1 hour and 24 hours later from the apical chambers. After separation by SDS–polyacrylamide gel electrophoresis (SDS-PAGE), the amount of biotinylated albumin in the apical chambers was visualized with a streptavidin probe. A molecular weight marker of 75 kD is indicated. (**B**) Transmission electron micrographs of two junctional areas in an MDCK cell monolayer infected with *H. pylori* (Hp) for 3 days, and fixed in the presence of the electron-dense dye ruthenium red. (**C**) MDCK cells infected before junction formation with wild-type (WT) or ΔCagA *H. pylori*. After 24 hours of infection, formation of functional tight junctions was determined by ruthenium red exclusion from the basal-lateral space. Arrows point to the location of tight junctions. Arrowheads show comparative ruthenium red staining of basal-lateral membranes. Scale bar, 0.25 μm.

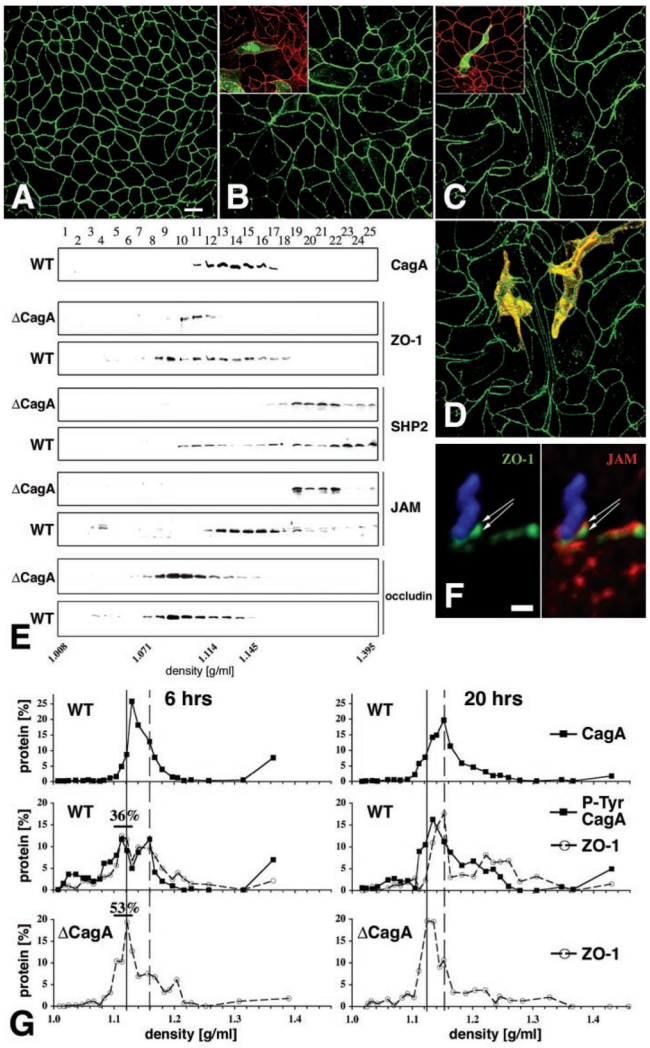

Fig. 4.

Effects of *H. pylori* infection on MDCK morphology and molecular organization of the apical-junctional complex. [(A) to (D)] Confluent monolayers of MDCK cells were infected with either nonadherent *H. pylori* (**A**), Δ*cagA* (**B**), or wild-type *H. pylori* (**C**) in continuous coculture for 7 days. Confocal immunofluorescence imaging of ZO-1 with an antibody to ZO-1 (green) outlines the shape of cell borders. (**D**) Optical sections of phalloidin staining (yellow) of actin were used to reconstruct the 3D shape of two cells within the monolayer infected with wild-type *H. pylori*. Similar experiments were done on a mixture of normal and GFP-expressing MDCK cells [insets in (B) and (C)]. Cells infected for 1 day with either wild-type [(C) inset] or Δ*cagA* [(B) inset] *H. pylori* were stained with anti–ZO-1 antibodies (red). The shape of single cells within the monolayer is revealed by GFP (green). (**E**) Membrane fractionation using 10–20–30% step iodixanol gradients. MDCK monolayers were infected for 5 days with wild-type or Δ*cagA H. pylori*. Twenty-five fractions of increasing density were separated by SDS-PAGE and the presence of CagA, ZO-1, SHP2, JAM, and occludin was determined by Western blot with appropriate antibodies. (**F**) Confocal immunofluorescence 3D reconstruction of an *H. pylori* (blue) adhered to the AGS cell surface for 4 hours and stained with antibodies to ZO-1 (green) and JAM (red). (**G**) Quantitative protein analysis of membrane fractions from MDCK cells during synchronized

junction assembly. Bacteria and calcium were added simultaneously to noncontacting cells and incubated for 6 or 20 hours. Membrane fractions separated by density were subjected to SDS-PAGE and analyzed by Western blot for CagA, ZO-1, and phosphotyrosine. Protein distribution is plotted as the percentage of total signal for each protein. Percentages of ZO-1 at 6 hours represent the sum of protein signals between 1.104 and 1.130 g/ml (black bars). Solid line, lighter peak; dashed line, denser peak.